Supporting Information

Xyloglucan-functional latex particles via RAFT-mediated emulsion polymerization for the biomimetic modification of cellulose

Fiona L. Hatton,[a] Marcus Ruda,[b] Muriel Lansalot,[c] Franck D'Agosto,[c] Eva Malmström[a] and Anna Carlmark[a]*

[a]*KTH Royal Institute of Technology, School of Chemical Science and Engineering, Department of Fibre and Polymer Technology, Teknikringen 56, SE-100 44 Stockholm, Sweden*
[b]*CelluTech AB, Teknikringen 38, SE-114 28 Stockholm, Sweden*
[c]*Université de Lyon, Univ Lyon 1, CPE Lyon, CNRS, UMR 5265, C2P2 (Chemistry, Catalysis, Polymers & Processes), Team LCPP, Bat 308F, 43 Bd du 11 Novembre 1918, 69616 Villeurbanne, France*

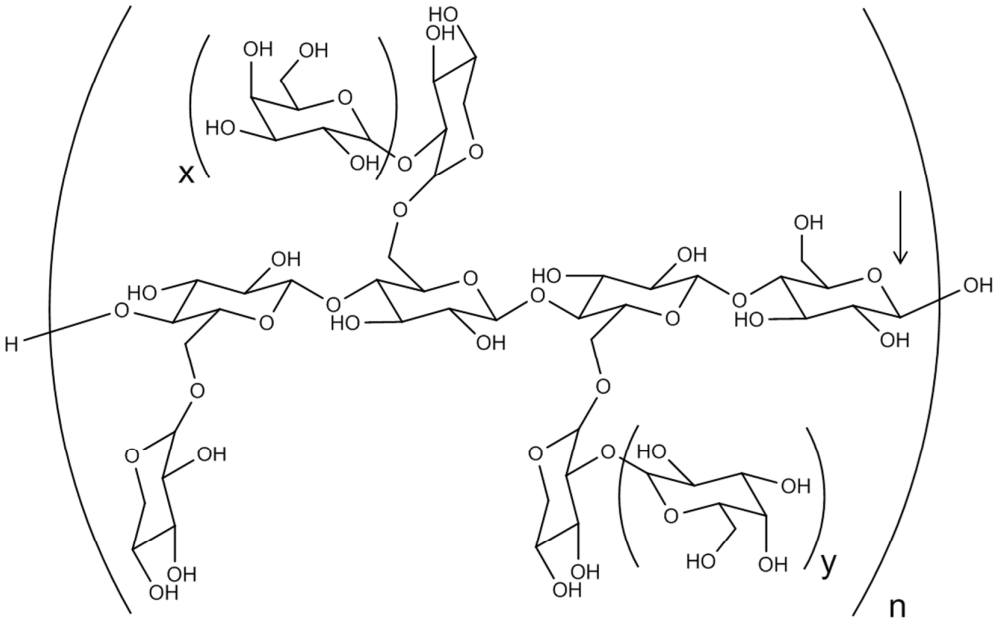

Figure S1. The structure of XXXG-type xyloglucans. Tamarind seed xyloglucan is comprised of XXXG (x = 0, y = 0), XLXG (x = 1, y = 0), XXLG (x = 0, y = 1), and XLLG (x = 1, y = 1).[1] The arrow indicates the reducing chain end.

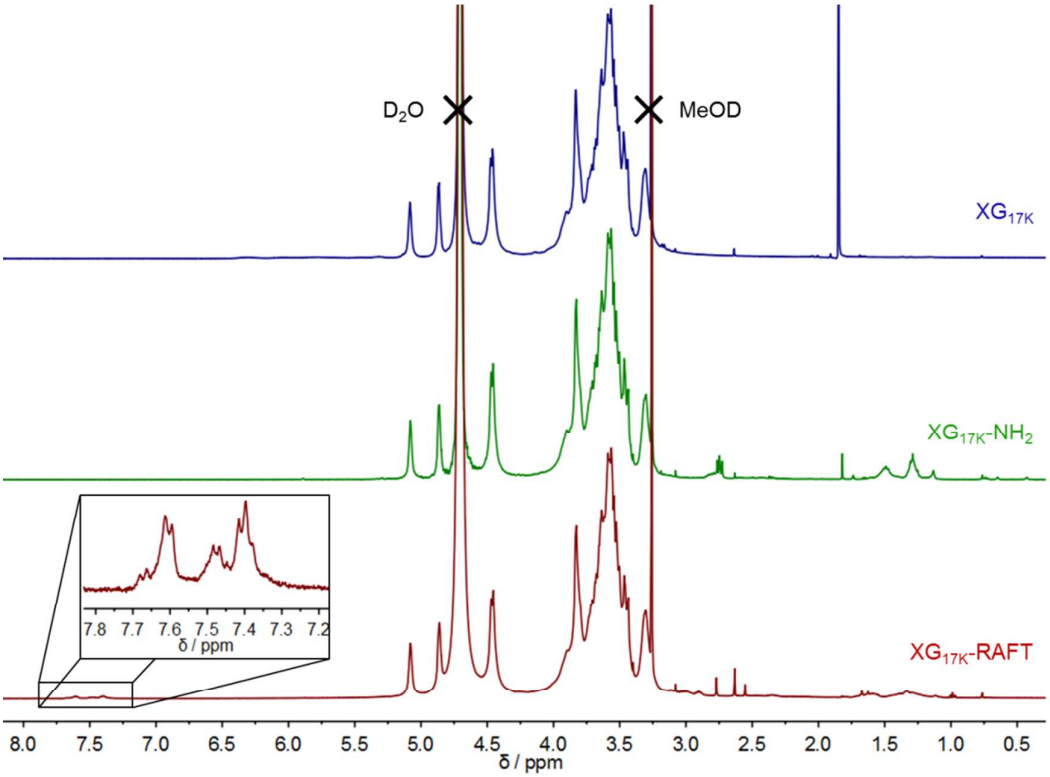

Figure S2 ^{1}H NMR (D_2O, 300 MHz) spectra overlay for XG_{17K}, XG_{17K}-NH_2 and XG_{17K}-RAFT. Expansion of the XG_{17K}-RAFT spectrum between 7.8-7.2 ppm shows the aromatic protons from the benzene ring present in the CTP RAFT moiety.

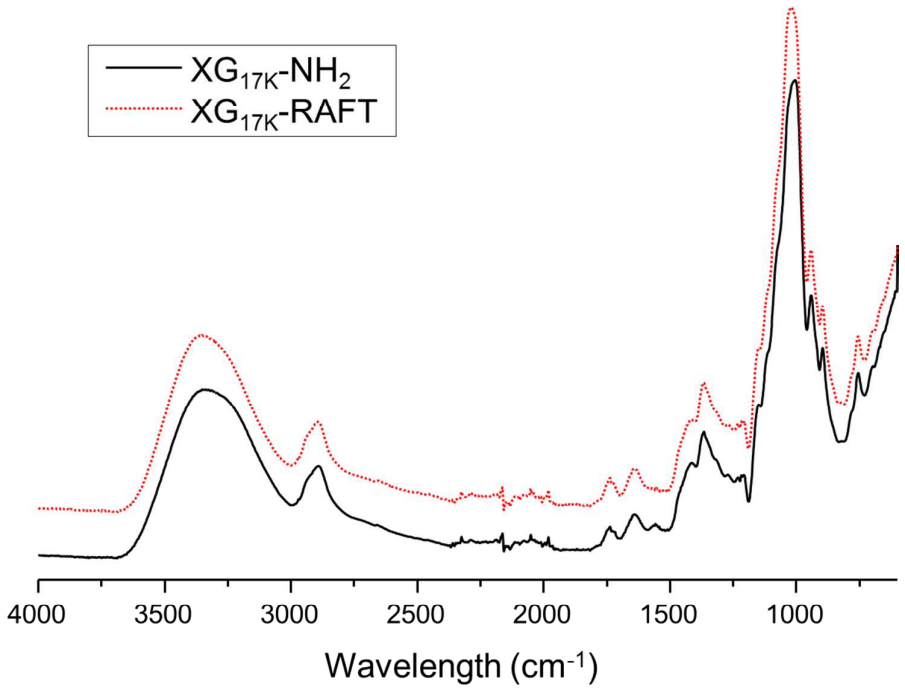

Figure S3 FT-IR spectra of XG_{17K}-NH_2 and XG_{17K}-RAFT

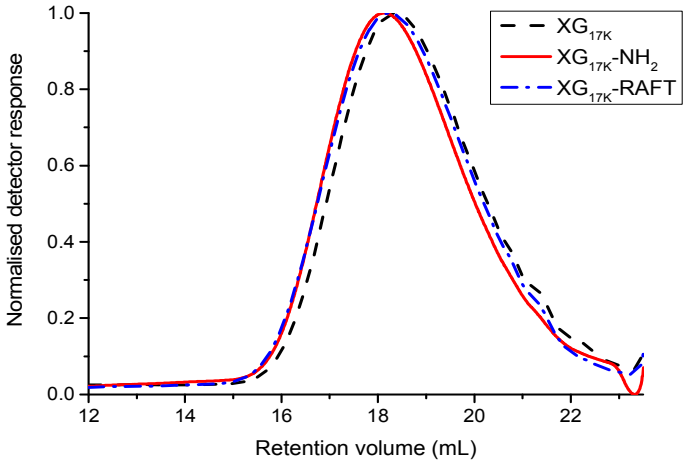

Figure S4 SEC (DMSO + 0.5 w/w% LiBr) chromatograms for XG_{17K}, XG_{17K}-NH_2 and XG_{17K}-RAFT

Table S1 SEC data for XG_{17K}, XG_{17K}-NH_2 and XG_{17K}-RAFT

	M_n (kg mol^{-1})	M_w (kg mol^{-1})	$Đ_M$
XG_{17K}	9.9	28.6	2.9
XG_{17K}-NH_2	12.0	33.0	2.8
XG_{17K}-RAFT	11.4	32.5	2.9

Mobile phase of DMSO + 0.5 w/w% LiBr using conventional calibration with pullulan standards

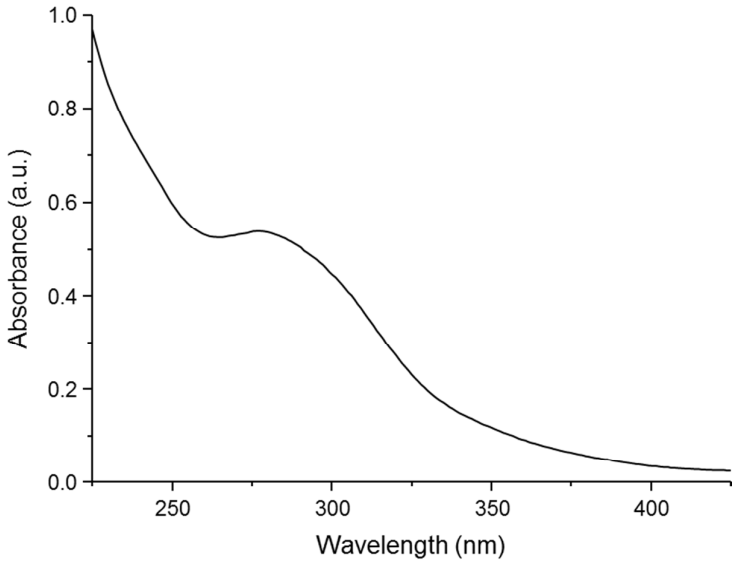

Figure S5 UV-visible spectrum of XG_{17K}-RAFT at 5 mg mL^{-1} in deionized water

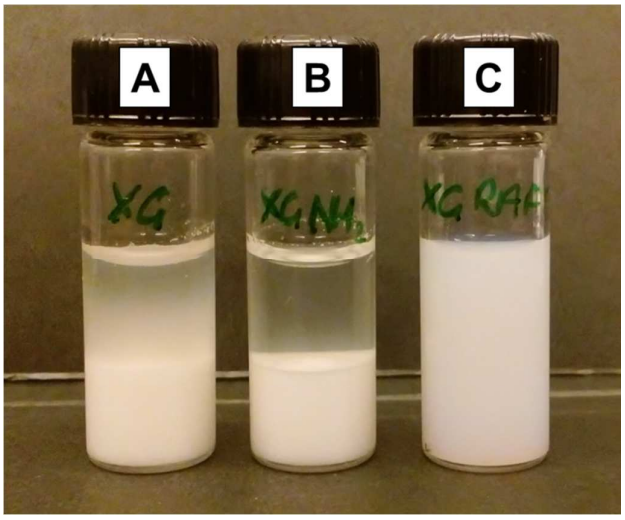

Figure S6 Photograph of samples conducted with the same experiment conditions as the 5-XG_{17K}-$PMMA_{175}$ sample: A) blank experiment with XG_{17K}, B) blank experiment with XG_{17K}-NH_2 and C) with XG_{17K}-RAFT. 3 mL of each sample was added to a vial and the image was taken after standing for 24 hours at ambient temperature.

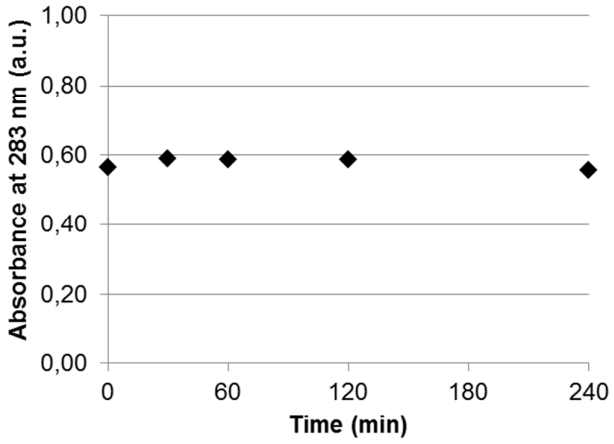

Figure S7 UV-Visible absorbance measured at 283 nm over time of the XG_{17K}-RAFT dissolved in deionized water (at a concentration of 5 mg mL^{-1}) at pH 6 and heated to 70 °C for 4 hours.

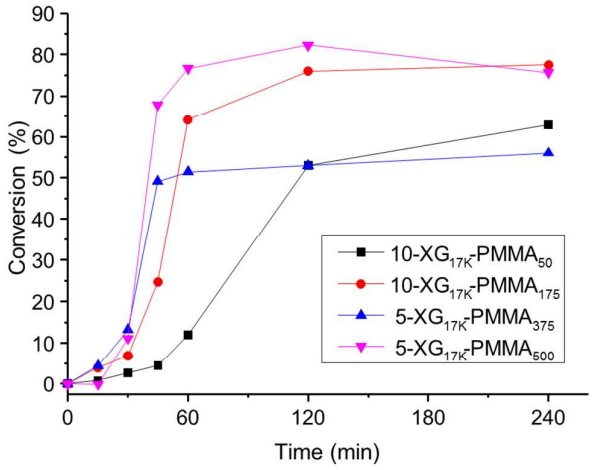

Figure S8 Kinetic evaluation of the RAFT-mediated surfactant-free emulsion polymerizations as conversion *vs.* time plots for samples 10-XG_{17K}-$PMMA_{50}$, 10-XG_{17K}-$PMMA_{175}$, 5-XG_{17K}-$PMMA_{375}$ and 5-XG_{17K}-$PMMA_{500}$.

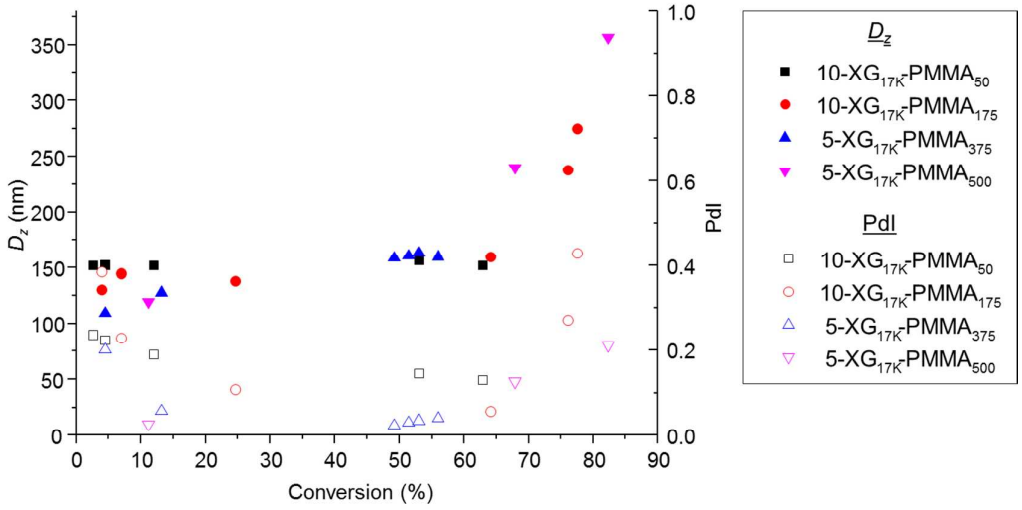

Figure S9 DLS measurements over time for samples 10-XG_{17K}-$PMMA_{50}$, 10-XG_{17K}-$PMMA_{175}$, 5-XG_{17K}-$PMMA_{375}$ and 5-XG_{17K}-$PMMA_{500}$. Closed symbols represent the z-average diameter (D_z) and open symbols the polydispersity index (PdI).

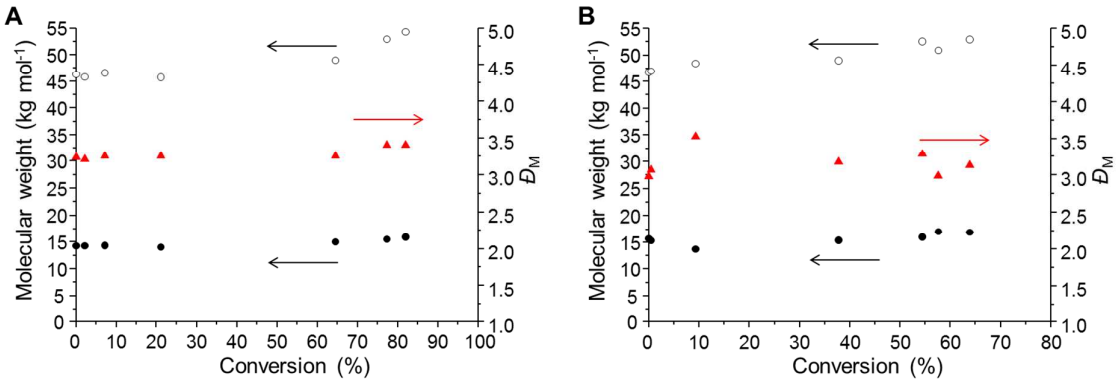

Figure S10 SEC data for the kinetic evaluation of A) 10-XG_{17K}-$PMMA_{100}$ and B) 5- XG_{17K}-$PMMA_{100}$. M_n (closed circles), M_w (open circles) and $Đ_M$ (triangles).

Table S2 DLS measurements for the XG_{17K}-$PMMA_x$ latexes prepared *via* aqueous RAFT emulsion polymerization

Sample name (τ-XG-$PMMA_x$)	MMA DP_{theor}	*Before dialysis*		*After dialysis*		
		D_z (nm)	PdI	D_z (nm)	PdI	ζ (mV)
10-XG_{17K}-$PMMA_{50}$	31	152	0.13	135	0.13	-7.1
10-XG_{17K}-$PMMA_{100}$	82	152	0.09	143	0.07	-3.6
10-XG_{17K}-$PMMA_{175}$	136	275	0.43	396*	0.75*	-1.4
5-XG_{17K}-$PMMA_{100}$	64	125	0.05	120	0.07	-5.6
5-XG_{17K}-$PMMA_{175}$	114	145	0.06	144	0.03	-5.9
5-XG_{17K}-$PMMA_{250}$	163	154	0.03	155	0.04	-7.2
5-XG_{17K}-$PMMA_{375}$	210	160	0.04	157	0.04	+3.1
5-XG_{17K}-$PMMA_{500}$	378	545*	0.49*	320	0.57	+2.5

*These samples failed on the DLS criteria, therefore they are too disperse for an accurate measurement.

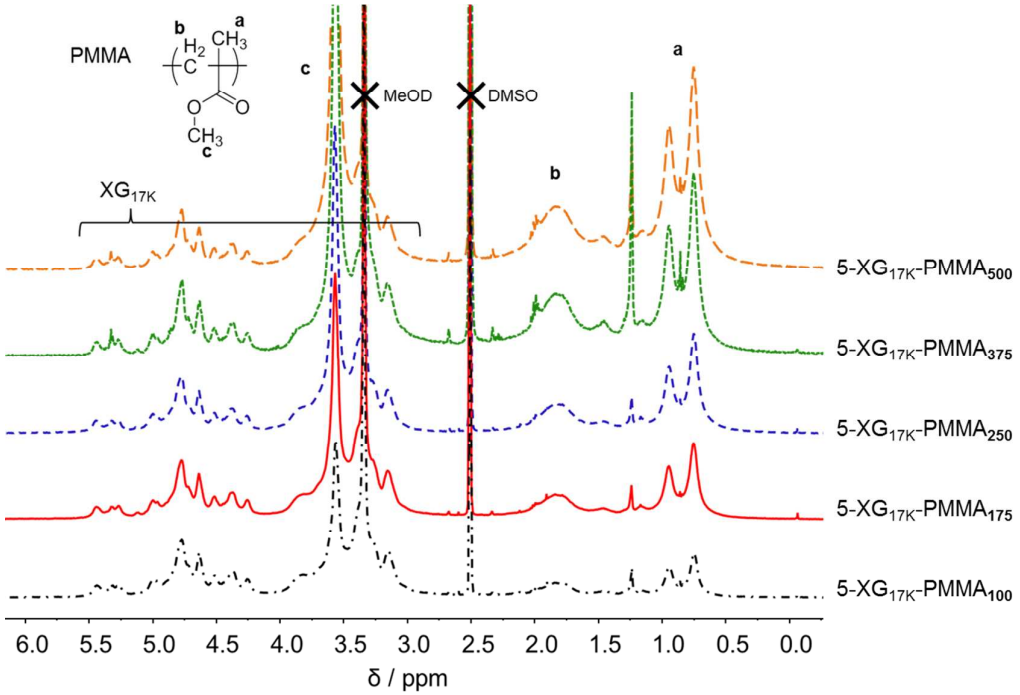

Figure S11 ^{1}H NMR (400 MHz, d_6-DMSO) spectra for the 5-XG_{17K}-$PMMA_x$ samples

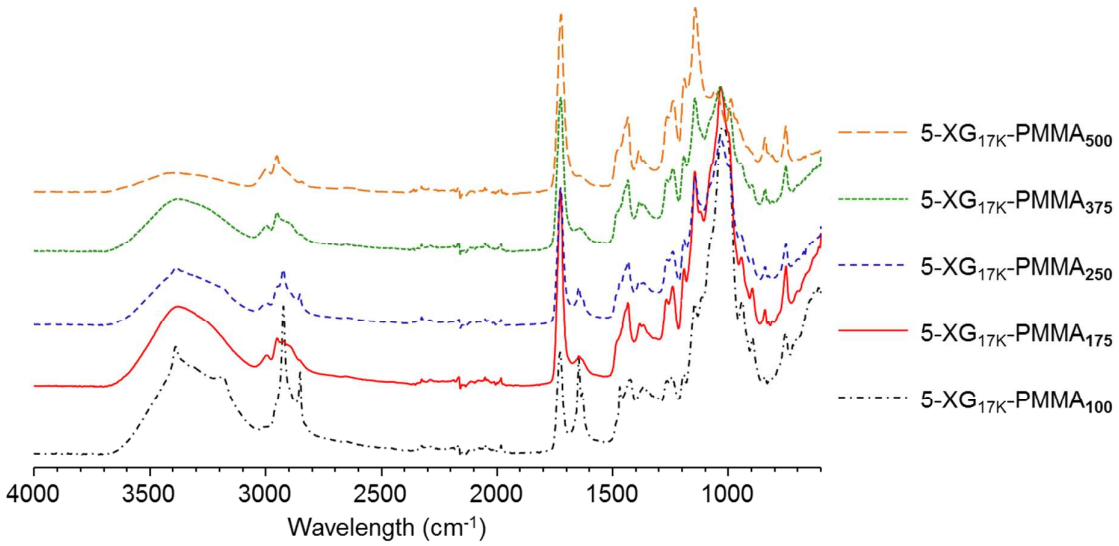

Figure S12 FT-IR spectra for 5-XG_{17K}-$PMMA_x$ dried latexes

Table S3 Thermal properties of the XG_{17K}-PMMA latex particles; thermal stability as assessed by the temperature at which 50 %wt loss was observed and the T_g of the samples

Sample name (τ-XG-PMMA$_x$)[a]	MMA DP_{theor}	Temperature at 50 %wt loss (°C)	T_g(°C)
$PMMA_{500}$[b]	500	366.2	122.9
XG_{17K}-RAFT	-	318.8	-
10-XG_{17K}-$PMMA_{50}$	31	324.0	123.4
10-XG_{17K}-$PMMA_{100}$	82	337.6	125.3
10-XG_{17K}-$PMMA_{175}$	136	347.7	126.9
5-XG_{17K}-$PMMA_{100}$	64	328.9	123.8
5-XG_{17K}-$PMMA_{175}$	114	339.5	127.5
5-XG_{17K}-$PMMA_{250}$	163	348.3	127.6
5-XG_{17K}-$PMMA_{375}$	210	354.4	127.7
5-XG_{17K}-$PMMA_{500}$	378	371.9	127.2

[a] τ = solids content, x = targeted DP. [b] $PMMA_{500}$ sample prepared by RAFT polymerization conducted in THF utilizing 4-cyano-4-(phenylcarbonothioylthio)pentanoic acid (CTP) as the RAFT agent.

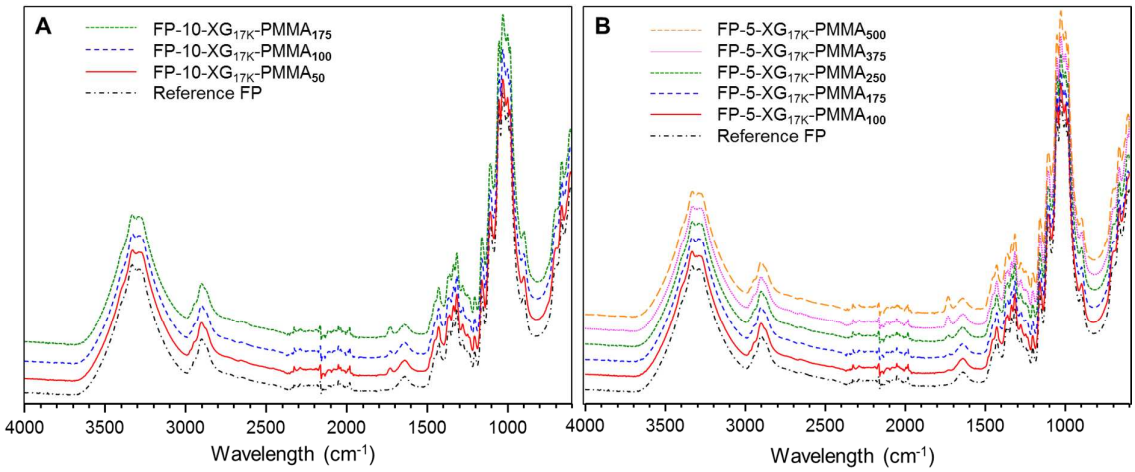

Figure S13 Full FT-IR spectra for filter papers after adsorption of the XG_{17K}-$PMMA_x$ latexes: A) the FP-10-XG_{17K}-$PMMA_x$ samples and B) the FP-5-XG_{17K}-$PMMA_x$ samples, corresponding to Fig. 3A and B in the main text.

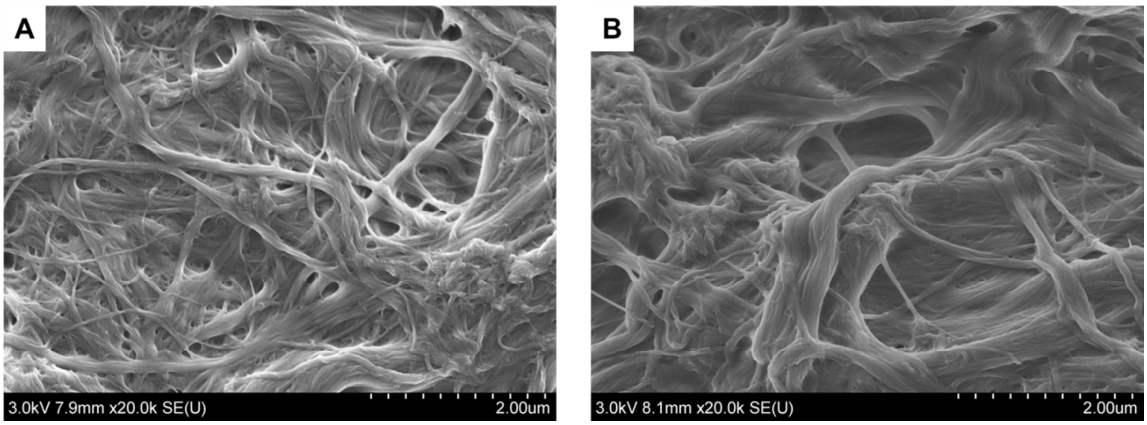

Figure S14 SEM images of the reference filter paper A) before and B) after annealing (160 °C, 1 h)

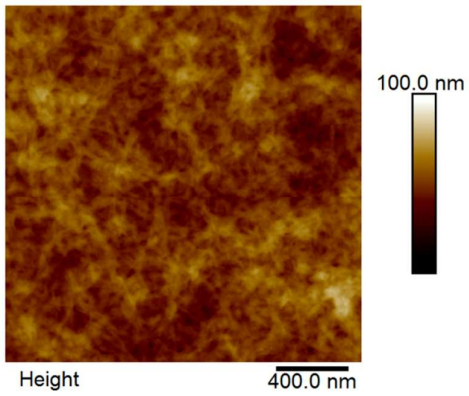

Figure S15 AFM height image of a cellulose model surface, R_q value of 7.8 ± 0.3 nm.

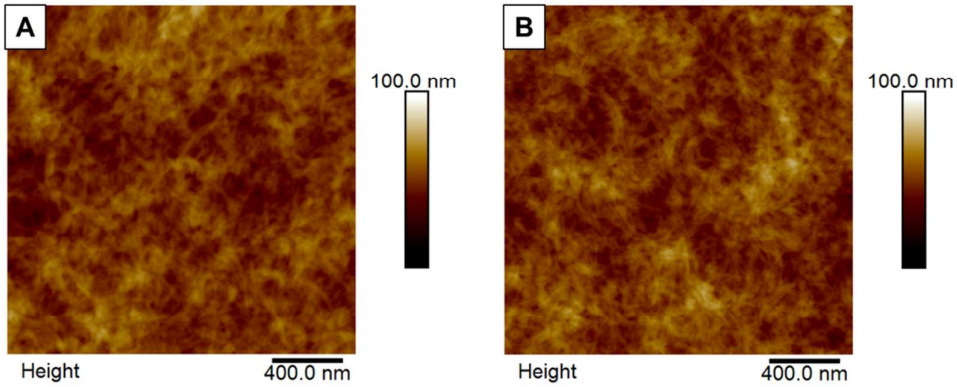

Figure S16 AFM height images of XG_{17K}-RAFT adsorbed onto a cellulose model surface; A) after adsorption and B) after annealing (160 °C, 1 h).

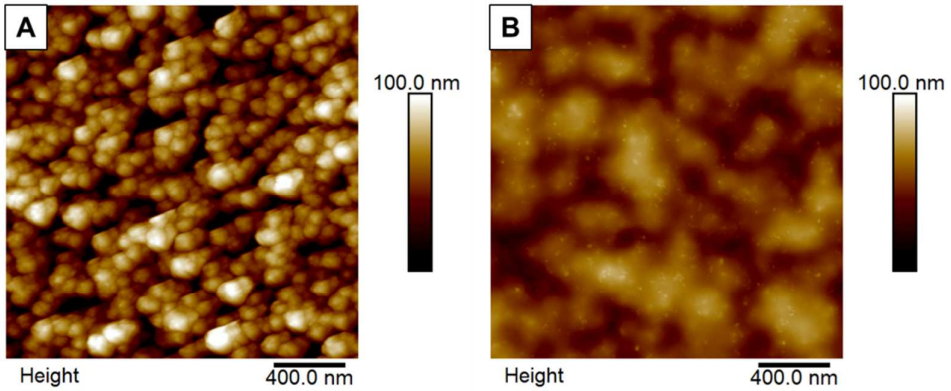

Figure S17 AFM height images of latex sample 5-XG_{17K}-$PMMA_{175}$ (Q3) adsorbed onto a cellulose model surface; A) after adsorption and B) after annealing at 160 °C for 1 hour.

1. Zhou, Q.; Rutland, M. W.; Teeri, T. T.; Brumer, H., *Cellulose* **2007,** 14, 625-641.